48th AIAA Aerospace Sciences Meeting Including the New Horizons Forum and Aerospace Exposition
4 - 7 January 2010, Orlando, Florida

AIAA 2010-728

Direct Numerical Simulations of Plunging Airfoils

Yves Allaneau[*] and Antony Jameson[†]

Stanford University, Stanford, California, 94305, USA

This paper presents the results of flow computations around plunging airfoils using a low dissipation finite volume scheme that preserves kinetic energy. The kinetic energy preserving scheme is briefly described and numerical experiments are done on low Mach, low Reynolds numbers plunging airfoils. Results are discussed and compared with experimental data.

Nomenclature

Re	Reynolds Number	κ	Coefficient of heat conduction
Pr	Prandtl Number	C_p	Specific Heat
M	Mach Number	L	Chord Length
Sr	Strouhal Number, $\omega h L / V_\infty$	h	Nondimensional Plunge Amplitude
x	Spatial Coordinate	ω	Angular frequency
t	Time variable	$\tilde{k}$	Reduced frequency, $\omega L / V_\infty$
v^i	i^{th} component of flow velocity	Ω	Fixed spatial domain
V_∞	Freestream velocity	$\partial\Omega$	Boundary of the domain Ω
ρ	Density		
p	Pressure		*Superscript*
E	Total Energy	i, j	Coordinate directions
H	Specific Total Enthalpy		*Subscript*
k	Specific Kinetic Energy	o, p	Grid Locations
μ	Dynamic Viscosity	∞	Far field quantity
λ	Volume Viscosity		

I. Introduction

Over the last century, steady airfoils have been thoroughly studied yielding important experimental and numerical results. On the contrary, unsteady flows around airfoils have not been well characterized due to their higher complexity. It is still a challenge to obtain accurate empirical data and current computational capabilities are not sufficient to gain high resolution of the phenomenon. In recent years, unsteady airfoils have been gaining a lot of interest, especially towards the use of flapping flight in the development of micro unmanned aircraft vehicles (UAVs).

The flow around a plunging airfoil is characterized by the generation of vortices that strongly interact in the wake of the airfoil. In order to study such an unsteady flow numerically and capture the phenomena present in the wake with good resolution, it is crucial to use a scheme that introduces as little dissipation as possible. When the artificial dissipation of the scheme becomes too large, there is significant uncertainty whether the damping observed is due to natural viscosity or numerical dissipation.

Jameson recently proposed a scheme that could overcome this problem. In his Kinetic Energy Preserving (KEP) scheme, the global balance of kinetic energy over the computational domain, along with the balance of mass, momentum and total energy is respected. The KEP scheme provides improved stability, removing almost completely the need of adding artificial viscosity and making it the best candidate for this study.

In this work, we used the KEP scheme to perform computations of flows around plunging airfoils at low Mach and low Reynolds number. Section 2 of this paper briefly describes the Kinetic Energy Preserving

---

[*]Graduate Student, Department of Aeronautics and Astronautics, Stanford University, AIAA Member.
[†]Professor, Department of Aeronautics and Astronautics, Stanford University, AIAA Member.

scheme developed by Jameson and the formalism used to solve the equations. Section 3 describes how the computations were performed. In Section 4, results are presented and discussed.

II.   Kinetic Energy Preserving scheme for viscous flow

In a recent paper, Jameson[1,2] presented a new semi-discrete finite volume scheme to solve the Navier-Stokes equations. This scheme has the property to satisfy the global conservation law for kinetic energy. We shall briefly describe this scheme in the present section.

II.A.   Continuous Model

First, consider the three-dimensional Navier-Stokes equations in their conservative form:

$$\frac{\partial u}{\partial t} + \frac{\partial}{\partial x^i} f^i(u) = 0 \tag{1}$$

where

$$u = \begin{bmatrix} \rho \\ \rho v^1 \\ \rho v^2 \\ \rho v^3 \\ \rho E \end{bmatrix} \quad \text{and} \quad f^i = \begin{bmatrix} \rho v^i \\ \rho v^i v^1 + p\delta^{i1} - \sigma^{i1} \\ \rho v^i v^2 + p\delta^{i2} - \sigma^{i2} \\ \rho v^i v^3 + p\delta^{i3} - \sigma^{i3} \\ \rho v^i H - v^j \sigma^{ij} - q^j \end{bmatrix} \tag{2}$$

The viscous stress tensor σ^{ij} is given for a Newtonian fluid by $\sigma^{ij} = \lambda \delta^{ij} \frac{\partial v^k}{\partial x^k} + \mu \left(\frac{\partial v^i}{\partial x^j} + \frac{\partial v^j}{\partial x^i} \right)$. Often in aerodynamics, λ is taken to be equal to $-\frac{2}{3}\mu$. The heat flux is proportional to the temperature gradient (Fourier's Law) $q^j = -\kappa \frac{\partial T}{\partial x^j}$.

An equation for the kinetic energy $k = \frac{1}{2}\rho v^{i^2}$ can be derived by combining the continuity and the momentum equations. Indeed,

$$\frac{\partial k}{\partial t} = \frac{\partial}{\partial t} \left(\frac{1}{2}\rho v^{i^2} \right)$$

$$= v^i \frac{\partial}{\partial t} \left(\rho v^i \right) - \frac{v^{i^2}}{2} \frac{\partial \rho}{\partial t}$$

It follows by substituting $\frac{\partial}{\partial t}\left(\rho v^i \right)$ and $\frac{\partial \rho}{\partial t}$ by their corresponding fluxes that:

$$\frac{\partial k}{\partial t} + \frac{\partial}{\partial x^j} \left[v^j \left(p + \rho \frac{v^{i^2}}{2} \right) - v^i \sigma^{ij} \right] = p\frac{\partial v^j}{\partial x^j} - \sigma^{ij} \frac{\partial v^i}{\partial x^j} \tag{3}$$

We assume that we are interested in a domain Ω fixed in space. $\partial\Omega$ denotes the boundary of Ω. By integrating (3) over the domain Ω, we get a global conservation law for kinetic energy.

$$\frac{\partial}{\partial t} \int_\Omega k \, dV = -\int_{\partial\Omega} \left[v^j \left(p + \rho \frac{v^{i^2}}{2} \right) - v^i \sigma^{ij} \right] n^j dS + \int_\Omega \left(p\frac{\partial v^j}{\partial x^j} - \sigma^{ij} \frac{\partial v^i}{\partial x^j} \right) dV \tag{4}$$

Definition 1 *A numerical scheme to solve the viscous Navier-Stokes equations is said to be Kinetic Energy Preserving if it satisfies a discrete analog of (4).*

Here we have assumed that the domain contains no discontinuity. If a shockwave is present in Ω, the relation (4) does not hold anymore.

American Institute of Aeronautics and Astronautics

II.B. Semi-discrete approach

Now, we consider a finite volume discretization of the governing equations in the domain Ω. The generic cell is a polyhedral control volume o. Each cell has one or more neighbors. The face separating cell o and cell p has an area A_{op}, and we define n_{op}^i to be the unit normal to this face, directed from o to p. Evidently $n_{op}^i = -n_{po}^i$. We also define $S_{op}^i = A_{op} n_{op}^i$. S_{op}^i can be interpreted as the projected face area in the coordinate direction i.

Boundary control volumes are closed by an outer face of directed area $S_o^i = -\sum_p S_{op}^i$ (a control volume is delimited by a closed surface).

In this framework, the semi-discrete finite volume approximation of the governing equations takes the form:

$$vol_o \frac{\partial u_o}{\partial t} + \sum_{p \text{ neighbor}} f_{op}^i \cdot n_{op}^i A_{op} = 0 \tag{5}$$

or

$$vol_o \frac{\partial u_o}{\partial t} + \sum_{p \text{ neighbor}} f_{op}^i \cdot S_{op}^i = 0 \tag{6}$$

For a boundary control volume b, another contribution to the fluxes $f_b^i \cdot S_b$ comes from the outer face.

Now we assume that u_o and f_{op}^i take the form:

$$u_o = \begin{bmatrix} \rho_o \\ \rho_o v_o^1 \\ \rho_o v_o^2 \\ \rho_o v_o^3 \\ \rho_o E_o \end{bmatrix} \quad \text{and} \quad f_{op}^i = \begin{bmatrix} (\rho v^i)_{op} \\ (\rho v^i v^1)_{op} + (p\delta^{i1} - \sigma^{i1})_{op} \\ (\rho v^i v^2)_{op} + (p\delta^{i2} - \sigma^{i2})_{op} \\ (\rho v^i v^3)_{op} + (p\delta^{i3} - \sigma^{i3})_{op} \\ (\rho v^i H)_{op} - (v^j \sigma^{ij} + q^j)_{op} \end{bmatrix} \tag{7}$$

Jameson has exhibited a set of sufficient conditions on the elements of f_{op}^i that lead to a Kinetic Energy Preserving (KEP) scheme.

Proposition 1 *If the elements of f_{op}^i defined in (15) satisfy the following conditions:*

a - $(\rho v^i v^j)_{op} = \frac{1}{2}(\rho v^i)_{op}(v_p^j + v_o^j)$

b - $(p\delta^{ij} - \sigma^{ij})_{op} = \frac{1}{2}(p\delta^{ij} - \sigma^{ij})_o + \frac{1}{2}(p\delta^{ij} - \sigma^{ij})_p$

and if the fluxes at the boundaries are evaluated such that:

c - $f_b^i = f^i(u_b)$ *where b is a boundary control volume*

then the semi discrete finite volume scheme (6) satifies the discrete global variation law for kinetic energy.

Indeed in that case, the discrete kinetic energy k_o satisfies the following relation:

$$\frac{d}{dt} \sum_o vol_o k_o = -\sum_b S_b^j \left(v_b^j \left(p_b + \rho_b \frac{v_b^{i\,2}}{2} \right) - v_b^i \sigma_b^{ij} \right)$$
$$+ \sum_o \left(p_o \sum_p \frac{v_o^i + v_p^i}{2} S_{op}^i - \sigma_o^{ij} \sum_p \frac{v_o^i + v_p^i}{2} S_{op}^i \right) \tag{8}$$

which is indeed a discretization of (4).

American Institute of Aeronautics and Astronautics

Condition a of the previous proposition is not very restrictive and allows some degrees of freedom in the construction of the fluxes defined in (15).

Let's denote by $\bar{g}_{op}$ the arithmetic average of the quantity g between cell o and cell p : $\bar{g}_{op} = (g_o + g_p)/2$. We can rewrite condition a

$$\left(\rho v^i v^j\right)_{op} = \left(\rho v^i\right)_{op} \bar{v}^j_{op} \tag{9}$$

We can evaluate the average $\left(\rho v^i\right)_{op}$ by any means ($\left(\rho v^i\right)_{op} = \bar{\rho}_{op}\bar{v}^i_{op}$ or $\overline{\rho v^i}_{op}$ for example) and then deduce $\left(\rho v^i v^j\right)_{op}$ by using (9) to satisfy condition a.

This degree of freedom could be used to design schemes that also satisfy other properties than Kinetic Energy Preservation.

III.   Direct Numerical Simulation of a plunging airfoil

The Kinetic Energy Preserving scheme described above was used to compute the flow around a plunging airfoil. Computations were done for a NACA 0012 airfoil oscillating in a uniform flow. The transversal motion of the airfoil is given by $h(t) = h \cdot cos(\omega t)$.
The freestream flow is characterized by a Mach number M_∞, a far field temperature T_∞ and a far field density ρ_∞.

Viscosity is evaluated using Sutherland's formula

$$\mu(T) = C\frac{T^{3/2}}{T + S}$$

For air, at reasonable temperatures, $C = 1.456 \times 10^{-6}\text{kg}/(\text{ ms}\sqrt{\text{K}})$ and $S = 110.4\text{K}$.

The Reynolds number is based on the chord length of the airfoil L and the free stream velocity $V_\infty = M_\infty c_\infty$

$$Re = \frac{\rho_\infty L V_\infty}{\mu_\infty} \quad \text{where } \mu_\infty = \mu(T_\infty) \tag{10}$$

The Prandtl number is given by

$$Pr = \frac{\mu C_p}{\kappa} \tag{11}$$

it was taken to be equal to 0.75.

Computational Domain

Simulations were done on a structured "C- mesh" counting 4096×512 cells. The computational domain extends roughly 30 chord lengths downstream and 20 chord lengths upstream, as can be see on **figure 2**. The mesh is subject to rigid body motion and moves with the airfoil.

Numerical fluxes

The convective fluxes have to be modified to account for the motion of the mesh. First, let us consider the hyperbolic system of equation (1) $\frac{\partial u}{\partial t} + \frac{\partial}{\partial x^i} f^i(u) = 0$ and integrate it over the moving domain $\Omega(t)$. We have using the divergence theorem

$$\int\limits_{\Omega(t)} \frac{\partial u}{\partial t}dV + \int\limits_{\partial\Omega(t)} f^i(u) \cdot n^i dS = 0 \tag{12}$$

However, since

$$\int\limits_{\Omega(t)} \frac{\partial u}{\partial t}dV = \frac{\partial}{\partial t}\int\limits_{\Omega(t)} udV + \int\limits_{\partial\Omega(t)} u\hat{v}^i \cdot n^i dS \tag{13}$$

American Institute of Aeronautics and Astronautics

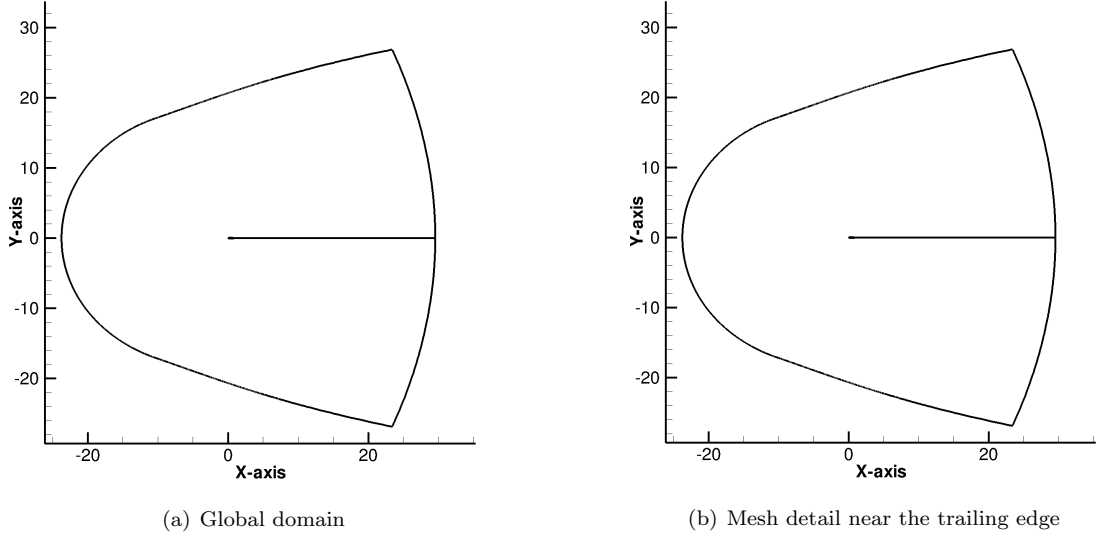(a) Global domain   (b) Mesh detail near the trailing edge

Figure 1. Computational domain

where $\hat{v}^i$ is the speed of the boundary of the domain, it follows that

$$\frac{\partial}{\partial t} \int\limits_{\Omega(t)} u dV + \int\limits_{\partial\Omega(t)} \left(f^i(u) - u\hat{v}^i \right) \cdot n^i dS = 0 \tag{14}$$

Denote $\hat{v}^i_{op}$ the velocity of the edge separating cells o and p. The convective fluxes, are now given by

$$f^i_{op \text{ convective}} = \begin{bmatrix} \left[\rho(v^i - \hat{v}^i_{op})\right]_{op} \\ \left[\rho(v^i - \hat{v}^i_{op})v^1)\right]_{op} + p_{op}\delta^{i1} \\ \left[\rho(v^i - \hat{v}^i_{op})v^2)\right]_{op} + p_{op}\delta^{i2} \\ \left[\rho(v^i - \hat{v}^i_{op})v^3)\right]_{op} + p_{op}\delta^{i3} \\ \left[\rho(v^i - \hat{v}^i_{op})E + pv^i\right]_{op} \end{bmatrix} \tag{15}$$

We then used the following averaging formula:

$$\begin{aligned} \left[\rho(v^i - \hat{v}^i_{op})\right]_{op} &= \overline{\rho}_{op}(\overline{v}^i_{op} - \hat{v}^i_{op}) \\ \left[\rho(v^i - \hat{v}^i_{op})v^j\right]_{op} &= \overline{\rho}_{op}(\overline{v}^i_{op} - \hat{v}^i_{op})\overline{v}^j_{op} \\ \left[\rho(v^i - \hat{v}^i_{op})E + pv^i\right]_{op} &= \overline{\rho}_{op}(\overline{v}^i_{op} - \hat{v}^i_{op})\overline{E}_{op} + \overline{p}_{op}\overline{v}^i_{op} \end{aligned} \tag{16}$$

Condition a of proposition (1) does not require a specific form for the energy flux. We defined it in a consistent manner with the continuity and momentum fluxes.
Viscous stress was evaluated in each cell by introducing a complementary mesh, for which cell vertices are the centers of the original control volumes.

Time integration

Time integration was done using a TVD Runge Kutta second order multistage time stepping scheme[3]. For a semi discrete law in the form

$$\frac{\partial u}{\partial t} + R(u, t) = 0 \tag{17}$$

American Institute of Aeronautics and Astronautics

the scheme advances from time n to time $n+1$ by

$$u^1 = u^n - \Delta t R(u^n, t^n)$$
$$u^{n+1} = \frac{1}{2}u^n + \frac{1}{2}u^1 - \frac{1}{2}\Delta t R(u^1, t^{n+1})$$

The explicit dependance in time of the operator R is due to mesh motion. This means that both the location and velocity of the mesh need to be updated at t^{n+1} before evaluating $R(u^1, t^{n+1})$.

This time discretization does not guarantee the preservation of kinetic energy in time. One could use a Crank-Nicholson semi implicit scheme as suggested by Jameson[1] to ensure conservation in time, but the computational costs would increase enormously.

Far field artificial dissipation

As the mesh coarsens in the far field, roughly 5 chord lengths away from the airfoil, small spurious oscillations associated with acoustic waves can be observed. It was shown in previous work[1,2,4] that the number of cells required to ensure a non oscillatory solution and stability was governed by the local cell Reynolds number, which has to be of the order of unity to guarantee these properties. However, covering the entire computational domain with cells as fine as the ones in the wake is currently too expensive.

A small amount of dissipation, based on the Jameson-Schmidt-Turkel (JST) scheme[7,8] was added in the far field to control these unphysical oscillations and prevent the explosion of the number of grid points. Furthermore, at the very edges of the computational domain, where the cells are the biggest, artificial dissipation is larger and behaves like a sponge that prevents the reflection of the acoustic waves into the computational domain.

The dissipation introduced in the far field was derived from the JST scheme by dropping the lower order diffusive term and conserving the higher order term to control odd/even modes. It shall be noted that no dissipation was introduced in the near field of the airfoil, an area encompassing about 70% of the cells. If we consider the conservation equation $\frac{\partial u}{\partial t} + \frac{\partial}{\partial x}f(u) = 0$, the truncation error introduced by our second order scheme can be seen as a continuous term in a modified differential equation

$$\frac{\partial u}{\partial t} + \frac{\partial}{\partial x}f(u) = O(\Delta x^2, \Delta t^2)$$

The idea is to introduce an extra diffusive term that will modify the truncation error

$$\frac{\partial u}{\partial t} + \frac{\partial}{\partial x}f(u) = -\Delta x^p \lambda^{(4)}\frac{\partial^4 u}{\partial x^4} + O(\Delta x^2, \Delta t^2)$$

with $\lambda^{(4)} \geq 0$ and $p \geq 2$ to preserve the order of the scheme. If

$$\frac{\partial u}{\partial t} + \frac{1}{\Delta x}\left[h_{i+\frac{1}{2}} - h_{i-\frac{1}{2}}\right] = 0$$

is a finite volume semi-discretization of the equation where $h_{i\pm\frac{1}{2}}$ is the numerical flux, we can introduce a correction $d_{i\pm\frac{1}{2}}$ to the flux to obtain the desired property. This can be done by taking

$$d_{i+\frac{1}{2}} = \alpha_{i+\frac{1}{2}}\epsilon^{(4)}\left(-u_{i+2} + 3u_{i+1} - 3u_i + u_{i-1}\right)$$

similarly to what is done in the JST scheme. $\alpha_{i+\frac{1}{2}}$ is proportional to the spectral radius of the local jacobian matrix and $\epsilon^{(4)}$ is a switch to add dissipation only where needed, as described in the original JST scheme. $d_{i+\frac{1}{2}}$ is proportional to $\Delta x^3 \frac{\partial^3 u}{\partial x^3}|_i$.

IV.   Results

We now present the results obtained using the numerical methods described above. We chose the various parameters describing the motion of the plunging airfoil to match the ones studied by Jones and Platzer[5,6]. Flows around plunging airfoils can be classified according to their Strouhal numbers $Sr = \frac{\omega h L}{V_\infty} = h\tilde{k}$. In all the results presented, the Mach number is taken to be $M_\infty = .2$ and the Reynolds number is $Re = 1850$.
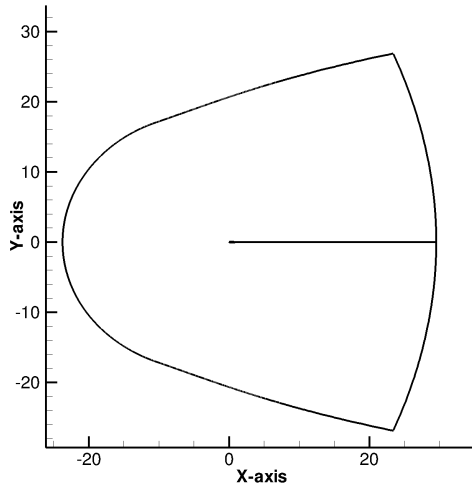
Figure 2. Artificial dissipation is added only in the darker area

Drag production at low Strouhal number - $Sr = 0.29$

The amplitude of the plunging motion is $h = 0.08$ and the reduced frequency $\tilde{k} = 3.6$ resulting in a Strouhal number $Sr = 0.288$. For such a Strouhal number the resulting flow exerts drag on the airfoil. Figure 3 shows the density contour: not only the flow pattern is clear on this picture, but this is also evidence that there are some non negligeable compressibility effects, even at such a low Mach number. Figure 4 represents the vorticity of the flow. As can be seen, the vortical structure of the wake is in agreement with the results obtained by Jones et al., cf. figure 5. Figure 6 is a plot of the evolution in time of the lift coefficient C_ℓ and the drag coefficient C_d. A positive C_d indicates that the fluid exerts drag on the airfoil in the flow direction. On the abscissa, the non dimensional time is defined by $\bar{t} = \frac{t}{t_0}, t_0 = \frac{L}{V_\infty}$.
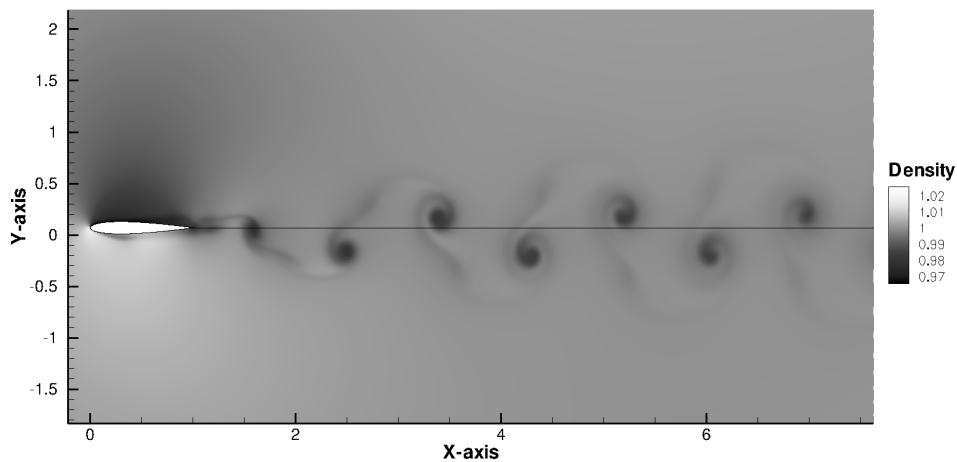
Figure 3. Density field in the airfoil's wake - $Sr = 0.29$

Thrust generation at high Strouhal number - $Sr = 0.60$

As the Strouhal number is increased the flow pattern changes and thrust is generated. In this section, we present the results obtained for a Strouhal number of $Sr = 0.60$. Figures 7 and 8 depict the computed density and vorticity fields for $h = 0.1$ and $\tilde{k} = 0.6$. The flow pattern is in excellent agreement with experimental

American Institute of Aeronautics and Astronautics
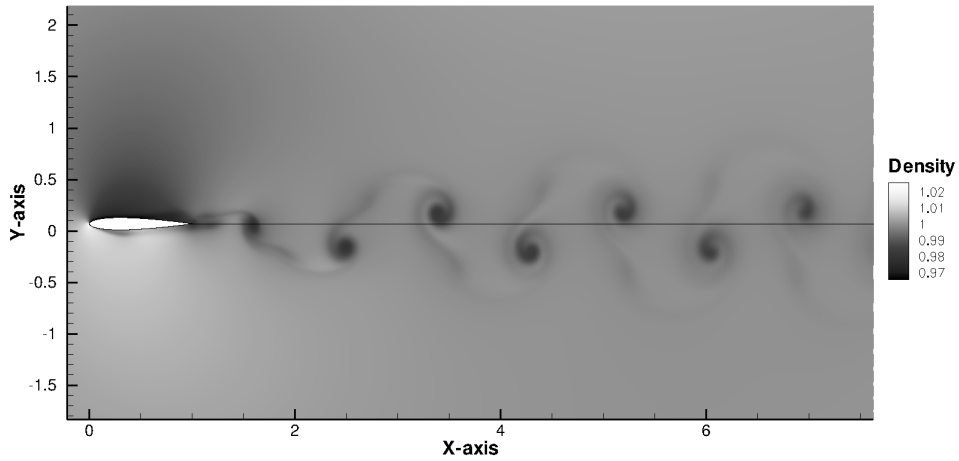
Figure 4. Vorticity distribution in the airfoil's wake - $Sr = 0.29$
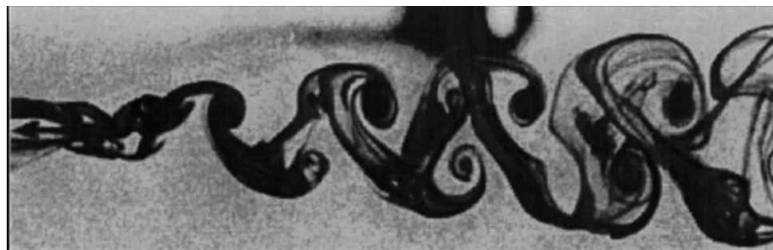

Figure 5. Streak lines, experimental data by Jones and Platzer - $Sr = 0.29$
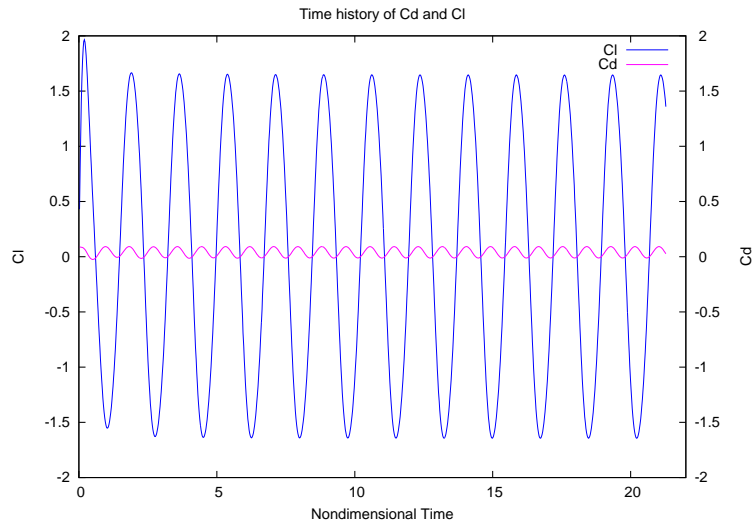

Figure 6. Lift and Drag history - $Sr = 0.29$

data by Jones et al. corresponding to this Strouhal number (see figure 9) and we observe on figure 10 that thrust is indeed generated. However, it should be noted that Jones' experimental result was obtained for $h = 0.2$ and $\tilde{k} = 0.3$. When we tried to compute the flow for these values, we still observed generation of thrust, but the flow pattern was quite different. The large amplitude of the motion (for $h = 0.2$) creates important leading edge vortices that interact strongly with the trailing edge vortices in the wake, as can be seen on figure 11.
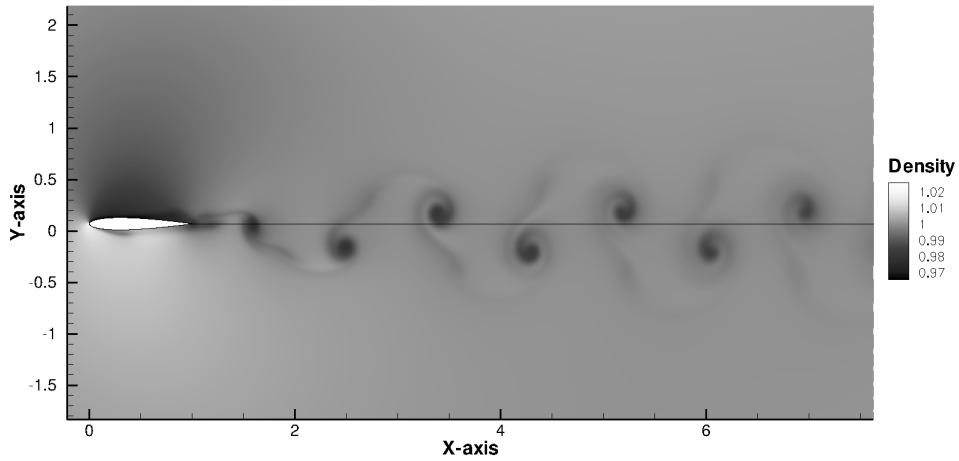
Figure 7. Density field in the airfoil's wake - $Sr = .60, \quad h = .1, \quad \tilde{k} = .6$
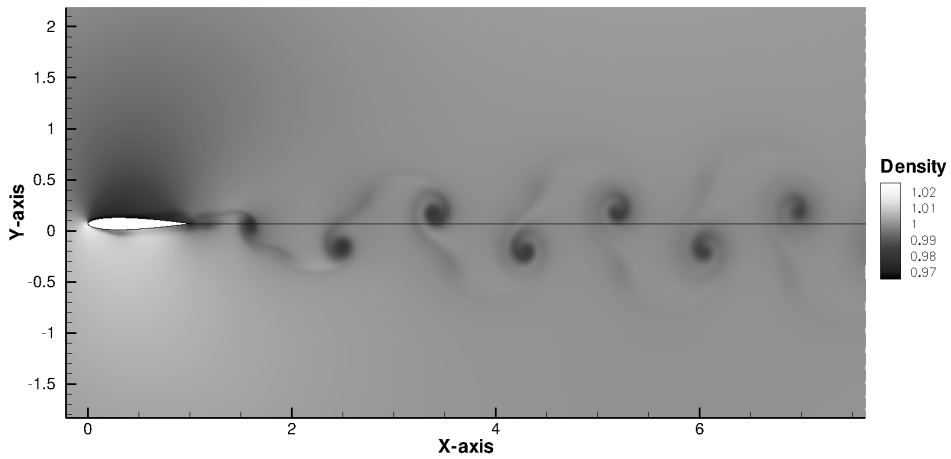
Figure 8. Vorticity distribution in the airfoil's wake - $Sr = .60, \quad h = .1, \quad \tilde{k} = .6$
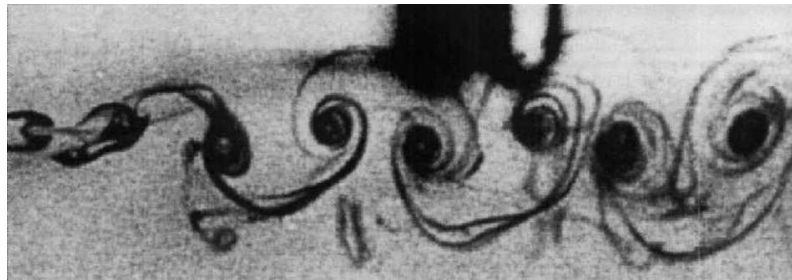

Figure 9. Streak lines, experimental data by Jones and Platzer - $Sr = 0.60, \quad h = .2, \quad \tilde{k} = .3$

Lift and thrust generation - $Sr = 1.5$

This is by far the most interesting case, as lift and thrust are generated by the oscillating airfoil. The nondimensional plunging amplitude is $h = .12$ and the reduced frequency $\tilde{k} = 12.3$, resulting in a Strouhal number $Sr = 1.48$. Figures 12 and 13 depict the density and the vorticity of the flow in the airfoil's wake. The dual-mode vortex street described by Jones et al.[5] is clearly visible. Our numerical computations are
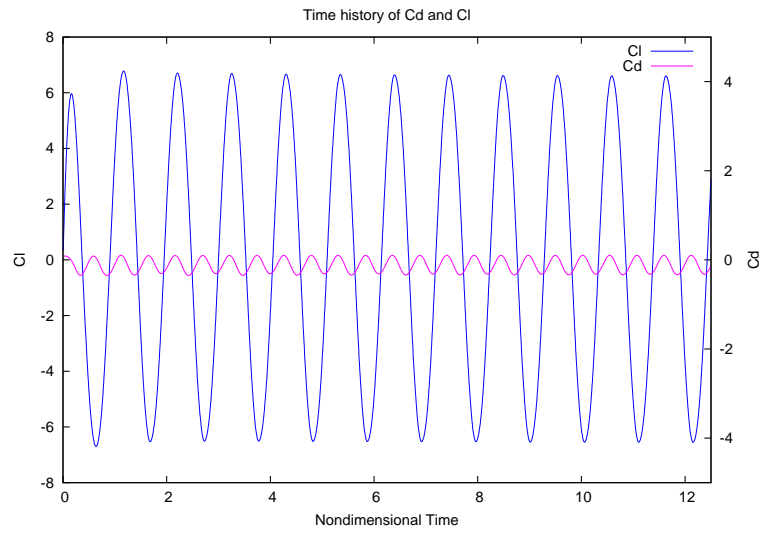
American Institute of Aeronautics and Astronautics

Figure 10. Lift and Drag history - $Sr = 0.60, \quad h = .1, \quad \tilde{k} = .6$
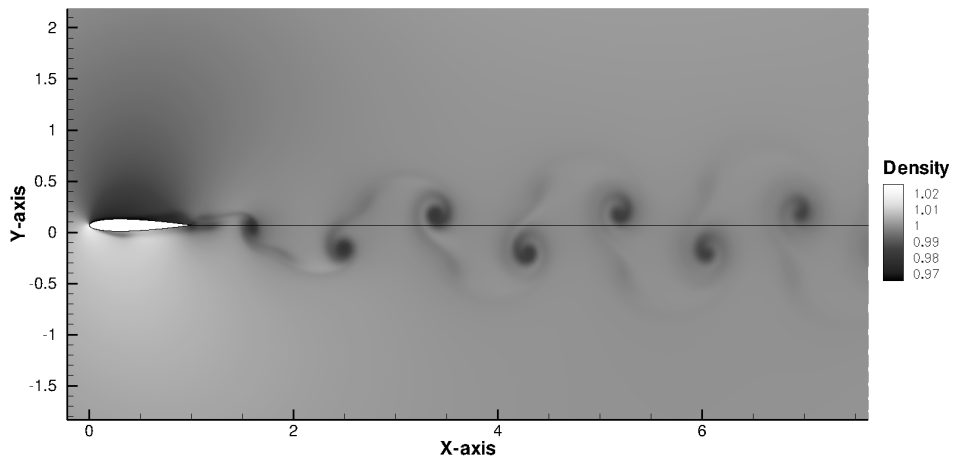

Figure 11. Vorticity field in the airfoil's wake - $Sr = .60, \quad h = .2, \quad \tilde{k} = .3$

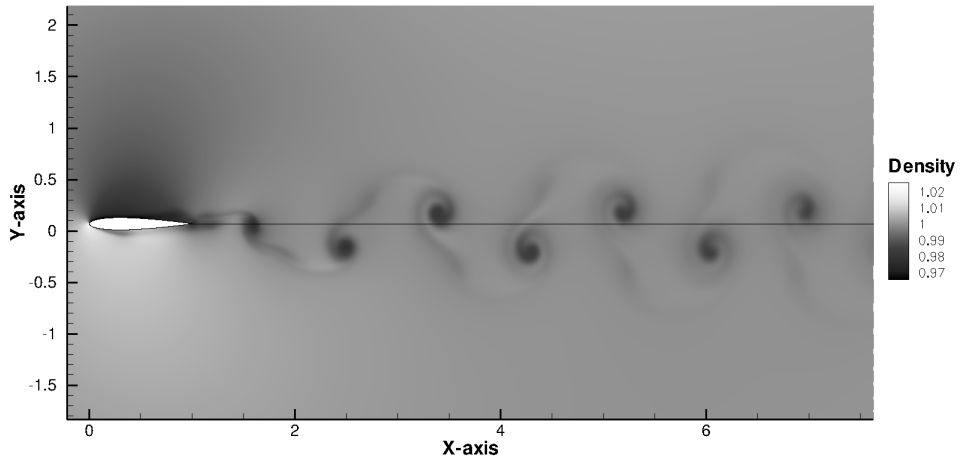again in excellent agreement with Jones et al. experimental results, as shown in figure 14.

American Institute of Aeronautics and Astronautics

Figure 12. Density field in the airfoil's wake - $Sr = 1.5$
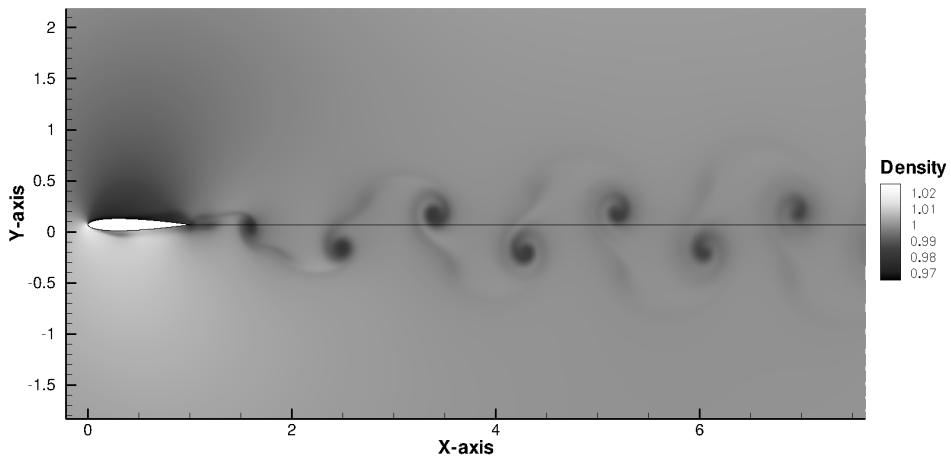

Figure 13. Vorticity distribution in the airfoil's wake - $Sr = 1.5$

Figure 14. Streak lines, experimental data by Jones and Platzer - $Sr = 1.5$

V.   Conclusion

This paper shows how to solve with high resolution the flow around plunging airfoils using a finite volume formulation. The method proposed uses the Kinetic Energy Preserving scheme proposed by Jameson and a
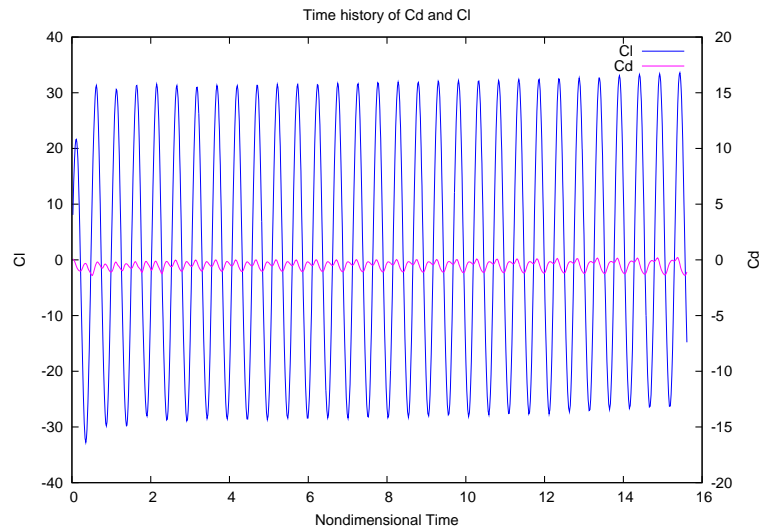
American Institute of Aeronautics and Astronautics

Figure 15. Lift and Drag history - $Sr = 1.5$

modified version of the JST artificial dissipation model in the far field to ensure a non oscillatory solution. The resulting code proved to be robust and extremely low dissipative. Applications with coarser grids containing "only" 1024×256 cells (results not presented in the present document) showed that even though the far field results were largely degraded, the time history curves of C_ℓ and C_d were still relatively close to the ones obtained with fine grids. On an other hand it appears that the code can be easily modified to deal with airfoil motions more complex, like a combination of pitching and plunging motion obeying non sinusoidal variations. These remarks lead us to think that this code would be particularly well suited in the study of optimal motions of rigid airfoils (in a sense of propulsion efficiency) at relatively low reynolds numbers.

Acknowledgments

References

[1] A. Jameson, The Construction of Discretely Conservative Finite Volume Schemes that Also Globally Converve Energy or Entropy, *Journal of Scientific Computing*, Vol. 34-2, p. 152-187, 2008

[2] A. Jameson, Formulation of Kinetic Energy Preserving Conservative Schemes for Gas Dynamics and Direct Numerical Simulation of One-Dimensional Viscous Compressible Flow in a Shock Tube Using Entropy and Kinetic Energy Preserving Schemes, *Journal of Scientific Computing*, Vol. 34-2, p. 188-208, 2008

[3] C. W. Shu, Total Variation Diminishing Time Discretizations, *SIAM Journal on Scientific and Statistical Computing*, Vol. 9, p. 1073-1084

[4] Y. Allaneau and A. Jameson, Direct Numerical Simulations of a Two-dimensional Viscous Flow in a Schocktube using a Kinetic Energy Preserving Scheme, *AIAA paper 2009-3797*, June 2009

[5] K. D. Jones, C. M. Dohring and M. F. Platzer, Experimental and Computational Investigation of the Knoller-Betz Effect, *AIAA Journal*, Vol. 36, No. 7, July 1998

[6] K. D. Jones, T. C. Lund and M. F. Platzer, Experimental and Computational Investigation of Flapping Wing Propulsion for Micro Air Vehicles, *Progress in Astronautics and Aeronautics*, Vol. 195, pp. 307-339. 2001

[7] A. Jameson, W. Schmidt and E Turkel, Numerical Solutions of the Euler Equations by Finite Volume Methods Using Runge-Kutta Time-Stepping Schemes, *AIAA paper 81-1259*, June 1981

[8] R. C. Swanson and E. Turkel, Artificial Dissipation and Central Difference Schemes for the Euler and Navier-Stokes Equations, *AIAA paper 87-1107*

American Institute of Aeronautics and Astronautics